IEEE Access
Multidisciplinary | Rapid Review | Open Access Journal

Received 19 September 2022, accepted 28 September 2022, date of publication 4 October 2022, date of current version 24 October 2022.

Digital Object Identifier 10.1109/ACCESS.2022.3211965

RESEARCH ARTICLE

Research on Forecasting Aeroengine Vibration Signals Based on the MAE Model

CUNJIANG XIA[1], YUYOU ZHAN[2], YAN TAN[1], AND WENQING WU[2]
[1]Aero-Engine Center Civil Aviation Flight University of China, Guanghan 618300 China
[2]College of Aeronautical Engineering, Civil Aviation Flight University of China, Guanghan 618300, China

Corresponding author: Yuyou Zhan (zyyskma@163.com)

This work was supported in part by the Key Research and Development Plan of Sichuan Provincial Department of Science and Technology under Grant 2022YFG0356, in part by the Key Research and Development Plan of Tibet Science and Technology Department under Grant XZ202101ZY0017G, in part by the CAAC Education and Training Program under Grant 0252001, and in part by the Fundamental Research Funds for the Central Universities under Grant J2022-014.

ABSTRACT For understanding the vibration states of aero-engines deeply and acquiring warning signs in real-time, a T-step forecast method of aero-engine vibration is proposed based on a powerful and advanced deep learning model, the MAE (Masked Autoencoders) model. Unlike previous common algorithms, the MAE model performs pre-training tasks by reconstructing information to achieve the purpose of analyzing and learning the latent information among parameters. Through the use of this technique, downstream tasks will be able to fine-tune and better suit the objective function, increasing the forecast's accuracy. Compared with simulation data and open-source datasets, this paper uses the real flight data recorded by aircraft data acquisition systems. This implies that the real vibration states of aero-engines can be learned and built. And from this, fairly practical conclusions can be reached. The result shows that it is feasible to forecast the vibration signal of aero-engines. This means that not only is that the first time series forecasting application of Transformer models that has a pre-training mechanism with masked code, but it also takes the lead in exploring the feasibility of vibration signal forecast in the aero-engine area. In addition, the possibility of forecasting in different types of aero-engines is also tested. Finally, to make our theories more reasonable and convincing, experiments on different aero-engine states involving the transition state and the steady state are carried out.

INDEX TERMS Aeroengine, vibration signal, vibration forecast, data driven, neural network.

I. INTRODUCTION

In civil aviation, aero-engine stability and safety are regarded as crucial aspects that guarantee a secure flight throughout the aircraft system. Due to increasing duty cycles, the performance of aero-engines will inevitably deteriorate [1]. This situation could cause severe vibration accidents because of malfunctions in aero-engines, such as being aged, corrosion and erosion in gas paths, blades worn out, and falling off between components [2], [3]. But the existing methods of fault diagnosis or prognosis on aero-engine suggest that a high accuracy could not be obtained because of human factors [4], [5]. And due to the complexity of aero-engines and the principle of confidentiality, there are often still obstacles to learning the operating law of critical systems as non-OEM (Original Equipment Manufacturer) [6], [7]. Not to mention that understanding the code of operation and potential developments of vibration helps airlines and non-OEMs gain a thorough understanding of aero-engine major systems. But as far as AI (Artificial Intelligence) that is based on data-driven methods is concerned, the techniques are more applicable and popular than traditional experiment-based methods. And it could be more appropriate to be used in quickly modeling key systems and obtaining analyzed data in time. Therefore, an effective AI system can make studying aero-engine vibration easier for airlines and non-OEMs.

With the advancement of sensors and material techniques, vital parameters have undergone more frequent monitoring in order to assess the functioning of aircraft engines. such as vibration signal levels, which have been affected by various

The associate editor coordinating the review of this manuscript and approving it for publication was Mostafa Rahimi Azghadi.

factors that are representative of the status of aero-engines in some way. Actual flight data captured by the sensors and simulation data are the two main dataset sources. While the simulation data could not fully adapt to the vibration signal setting [8], [9], the research on aero-engines makes extensive use of it. And this raises the question of whether the experimental findings are trustworthy and useful. The actual flight datasets generated from flights can solve the above problems. In addition, the research of the aero-engine vibration is only limited to fault diagnosis, fault prognosis, and flow forecast, but never involves forecasting tasks [10], [11], [12]. While looking deep into the forecast of the aero-engine vibration will bring huge positive feedback to the control system optimization and flight security. Particularly for those who are not original aero-engine designers but are researchers in this area, which could provide some inspiration for them. Therefore, it is extremely meaningful and practical to study the possibility of the aero-engine vibration forecast. On the basis of the above, using the data-based methods to study forecasting the vibration signal of aero-engines will provide a considerable degree of support for aero-engines design optimization and airworthiness safety monitoring, based on the above background.

In this paper, a new methodology is proposed for the possibility of the aero-engine vibration forecast based on the masked autoencoders (MAE) model and multi-parameters fusion. The datasets we used in this study are collected from aircraft data acquisition systems. It should be noted that the utility of this method is verified with the difference (MSE) between the actual vibration level and the forecasted one. Based on the above, we hope that our work will be able to expand research on how to accurately forecast the study object in the area of aero-engines. Our paper's novelty and contribution are as follows: I. This paper presents the feasibility of forecasting the vibration signal based on real flight datasets. This is a huge leap in the aero-engine vibration field. II. This article proposes an advanced application of the MAE model to time series prediction. The MAE model's usefulness in multiple target prediction tasks was also demonstrated by its remarkable theory, the pre-training task with the masked mechanism.

II. RELATED WORK

Deep learning has been observed and used to explore more complicated problems employing tens of thousands of large-scale datasets since the advent of AI and the advancement of computer technology. And due to its end-to-end pattern, deep learning algorithms can save the cost of manual feature extraction and design process [13], [14], [15], [16]. Because of its rapid modeling capability and wide applicability, deep learning is attracting the attention of aero-engine experts for use in pertinent studies.

The majority of research on aero-engine vibration focuses on baseline modeling, fault classification, and prognosis or diagnosis of failures. Dong et al. proposed an optimized convolution and bidirectional long short-term network, and it achieved a high accuracy rate(96.87%) on bearing fault diagnosis by using Case Western Reserve University bearing datasets [17]. Shao et al. used a deep belief network (DBN) and this method is superior in stability and accuracy to the traditional methods [18]. Zhang et al. combined auto-encoder (AE) and parameter transfer for bearing fault detection at variable rotating speeds [19]. And all of the references, from 10 to 12, deal with studies on bearing problem identification in a vibratory condition.

In particular, these analyses of aero-engine vibration have the following disadvantages. 1. The aspects of data. Current research on aero-engine vibration primarily uses laboratory simulation data, software simulation data, or open-source datasets. These data are limited to reflect the real condition of aero-engines. And it is produced in limited artificial conditions, thus the datasets are not perfect in some ways. There are several significant ways in which the actual flight data and simulated data diverge. In addition, aero-engines are more reliably and correctly represented by datasets collected under real flying conditions. 2. Limited parameters. In order to fully and accurately analyze the vibration code, it is necessary to study aero-engine vibration and collect parameters as comprehensively as possible. Some studies on aero engines have solely looked at the vibration parameters directly, ignoring other factors. The results are not sufficiently validated by this. On the other hand, because the aero-engine is a complex system, it is important to consider all relevant elements in as much detail as possible. 3. Controlled experiments. It's important to consider the effectiveness of various aero-engine types. The result will have less reliability and application if there is no such control experiment. 4. The study of forecasts is lacking. The significance of studying aero-engine vibration has been discussed in light of the background information provided above. The forecasting method's description, however, is still unclear. The majority of studies on fault diagnosis and failure prognosis analyze classification issues. Despite the fact that this is a serious issue, it belongs in the detection that follows a fault. The necessity for early fault detection can be met if the vibration is forecasted, but it can also aid in the research of the fundamental principles governing the entire vibration system. The most crucial part that can benefit non-OEM researchers and airlines is this one. As a result, it is important to pay more attention to forecasting the level of vibration signals.

III. DATA PREPROCESSING

A. DATA ACQUISITION

The primary methods of data acquisition can be listed as follow: simulation data, open-source datasets, and aircraft data acquisition systems. The datasets this paper used are the aircraft acquisition system's data generated from the actual flight. Compared with the traditional simulated data and the open-source datasets, the datasets we used could be better at mapping the operational status of aero-engine vibration. Various and detailed parameters, continuous storage, and easy

export and processing are all advantages of our datasets [20]. These characteristics make our study more reliable and complete. In addition, the types of aero-engines we studied are dual rotor engines, hence the data belong to the dual rotor engine.

It should be noted that the airborne vibration computer used to analyze the data for the vibration level studied in this article first filtered any unnecessary signals. Therefore, the vibration parameters recorded by the aircraft data acquisition system cannot obtain the frequency distribution of vibration, and only the vibration of the whole aero-engine rotor could be accessible. The vibration level processed by the airborne vibration computer is thus the forecasting target value obtained in this paper. Although it is unavailable to gather further information on vibration, such as modal distribution and response position, it also has certain practical significance and research value in aero-engines early warning, the design and research of aero-engines through the forecasting and tracking of future trends and sudden changes of vibration. Additionally, our research can serve as an inspiration for the study of vibration systems in other fields.

More significantly, there are two types of aero-engine operating conditions: steady state and transition state, which cover the entirety of a flight. As a result, conducting the experiment in several states is necessary following the overall experiment. Thankfully, this paper includes the relevant experiments. Meanwhile, datasets from both states will be randomly extracted and input into our model at the same time. When the model is sufficiently complex, it could learn the patterns of these two states in training tasks and identify which state it is according to the input data during the forecasting process. Then the trained model can be regarded as a general forecast model that does not need to distinguish aero-engine conditions in the data preprocessing part due to its automatic recognition capability.

B. PARAMETER SELECTION

This part will introduce the parameter selection of two different types of aero-engines we mainly studied. And the selection of these two types of aero-engines will try to stay the same. In the parameter selection, the interaction of factors will be concerned and based on the technology of aero-engines and the ability of data acquisition. In addition, by referring to the company's manual and previous aero-engine vibration papers, the following parameters will be chosen from the type B aero-engine and type A aero-engine [21], [22]. Table 1 shows the parameters chosen from type B aero-engine. The vibration level of low pressure compressor and the vibration level of high pressure compressor will be chosen as our target parameters.

For another type of aero-engine, the parameters that we chose from the type A aero-engine are the following. The vibration level of low pressure compressor and the vibration level of low pressure turbine will be chosen as our target parameters.

TABLE 1. Parameters selection (Type B).

Parameter	Unit
Vibration levels of low pressure compressor	MILS.DA
Vibration levels of high pressure compressor	MILS.DA
Vibration levels of low pressure turbine	MILS.DA
Vibration levels of high pressure turbine	MILS.DA
High pressure compressor outlet pressure (PS3)	PSIA
Fan inlet temperature (T12)	℃
High pressure compressor inlet temperature (T25)	℃
High pressure compressor outlet temperature (T3)	℃
Low pressure rotor speed (N1)	%RPM
High pressure rotor speed (N2)	%RPM

TABLE 2. Parameters selection (Type A).

Parameter	Unit
Vibration levels of low pressure compressor	MILS.DA
Vibration levels of high pressure compressor	MILS.DA
Vibration levels of low pressure turbine	MILS.DA
Vibration levels of high pressure turbine	MILS.DA
High pressure compressor outlet pressure (PS3)	PSIA
Total air temperature (TAT)	℃
High pressure compressor inlet temperature (T25)	℃
High pressure compressor outlet temperature (T3)	℃
Low pressure rotor speed (N1)	%RPM
High pressure rotor speed (N2)	%RPM

C. MISSING VALUES PROCESSING

In this paper, we compared the different interpolation methods such as linear, nearest, zero, quadratic, cubic and barycentric. Figure 1 shows the results of the above interpolation methods using the T3 factor in one flight. By contrast, each method does not have an impact on the general trend, but the linear is smoother. Consequently, the linear will be a good concern relatively. Figure 2 presents the comparison of complete data and raw data using the T3 factor in one flight.

D. THE TERM 'STEP'

It should be noted that the term 'step' has been used to refer to situations in which time series data are used. In the present study, a step is defined as the frequency of recording data. Particularly, one step can be representative of the sensor acquisition rate which is 1 Hz. This paper attempts to show the feasibility of predicting a vibration parameter in the next 10 steps using 100 step correlative parameters. Because the result is expected to provide better forecasting and tracking of vibration levels to ensure airworthiness.

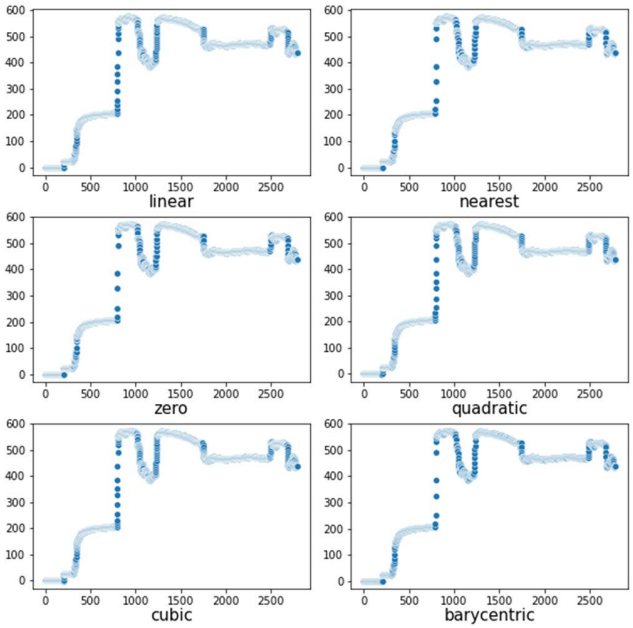

FIGURE 1. Comparison results of interpolation methods (Type A Aero-engine).

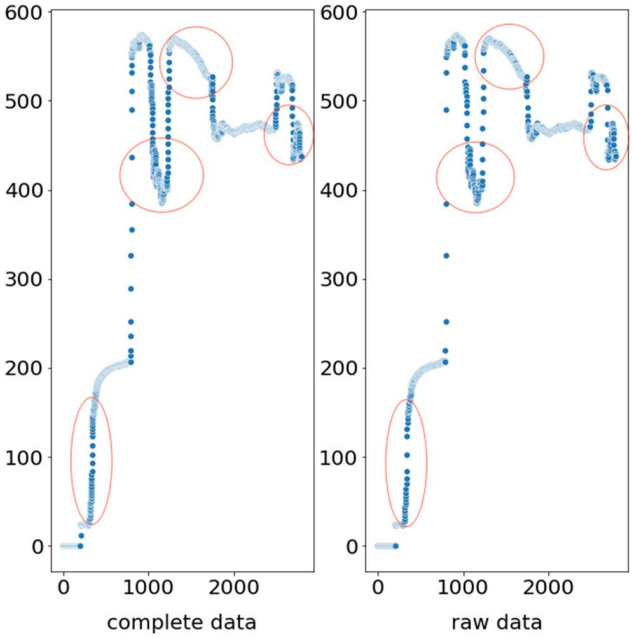

FIGURE 2. Comparison results of complete data and missing data (Type A Aero-engine).

E. RANDOMIZING DATA EXTRACTION

To build an accurate model, this paper extracts data randomly. This technique will help our model to learn more suitable parameters, which will fit the real latent vibration function better. And the model would learn the interaction of relevant vibration factors rather than the sequential relation of parameters in flight sectors [23], [24]. One batch consists of 100 continuous steps as input values and 10 uninterrupted steps as output values. In the fourth section, we will randomly sample 64 batches as the input to a round of training.

IV. MODEL ARCHITECTURE

In recent years, Transformers, which are self-attention-based architectures, have become a common choice in many natural language processing (NLP) tasks [25]. Especially with the advent of a conceptually simple and empirically powerful model, BERT which extends the structure of Transformers, the pre-training tasks are more effective in enhancing NLP learning tasks [26], [27]. And it shows the importance of bidirectional pre-training for language representations and makes the need for many task-specific architectures highly designed to be reduced as the first fine-tuning based representation model [28]. Furthermore, the use of Transformers has been extended from NLP to computer vision (CV). Masked autoencoders (MAE) are scalable self-supervised learners for CV, and the approach is clear: we just need to mask random patches of the input image and reconstruct the missing pixels [29]. And the original MAE architecture will be provided in Figure 3.

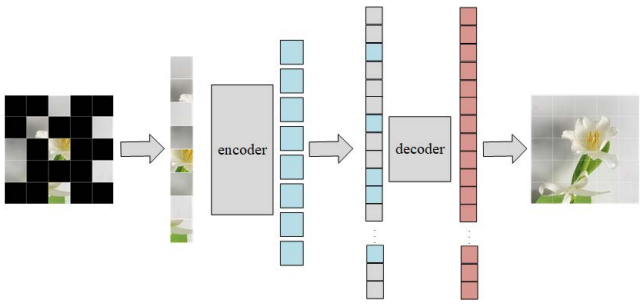

FIGURE 3. Original MAE architecture.

The MAE model consists of two key designs. Firstly, The entire architecture is asymmetric. Only The visible subset of patches (without mask tokens) will be input to the encoder, and a lightweight decoder will be appointed to reconstruct the original image from the latent representation and mask tokens. Secondly, a nontrivial and meaningful self-supervisory task will be yielded because a large proportion of the input has been masked, e.g., 75% [29] This challenging task generated by these two vital design ideas makes the MAE model more effective and efficient in training large models process. In addition, only a quarter of the original data will be input, hence the training speed is more than three times faster.

The MAE encoder is just a standard ViT [30] but applied only on visible, unmasked patches. The encoder uses a linear projection to embed patches and adds positional embeddings. The above process outputs will enter a number of Transformer blocks. Figure 4 below illustrates the Vit model. We noticed the beautiful characteristics of MAE encoders. Thus, according to these properties, the adaptability of aero-engine vibration prediction has been studied. The model might learn the latent relation of vibration factors because of the ambitious

and challenging pre-training. Moreover, the encoders could learn the important features due to the Transformer parts [25]. In addition, the result might be universal for other vibration parameters' prediction because of the pre-training which involved other vibration factors. Therefore, this architecture will further save computing costs.

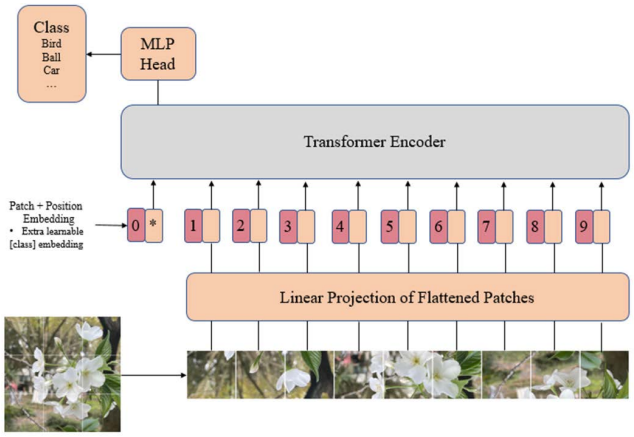

FIGURE 4. Vision transformer(ViT).

An overview of the ViT model is presented in Figure 4. In this architecture, the dimension of our data is $x \in \mathbb{R}^{H\times W\times C}$, and out data will be transformed into a sequence of flattened 2D patches $x \in \mathbb{R}^{N\times(P^2\cdot C)}$, where (H, W) is the time steps and features of out input. C is the number of channels that will be one in our study. (P, P) is the resolution of each image patch, and $N = HW/P^2$ is the resulting number of patches, which also serves as the effective input sequence length for the Transformer. In addition, constant vector size D through all of the Transformers' layers, hence MAE's authors flatten the patches and map to D dimensions with a trainable linear projection (Eq.1). For the MAE model, the output of this projection means the patch embeddings. Similar to BERT's [class] token, MAE add a learnable embedding to the sequence of embedded patches ($z_0^0 = x_{class}$), whose state at the output of the Transformer encoder (z_L^0) serves as the image representation y (Eq. 4) [30]. In our study, we could neglect it due to our objective is regression, not classification. And the Multilayer Perceptron (MLP) contains two layers with GELU non-linearity.

$$z_0 = \left[x_{class}; x_p^1 E; x_p^2 E; \cdots; x_p^N E\right] + E_{pos}$$
$$E \in \mathbb{R}^{(P^2\cdot C)\times D}, E_{pos} \in \mathbb{R}^{(N+1)\times D} \quad (1)$$
$$z'_\ell = MSA(LN(z_{\ell-1})) + z_{l-1}\ell = 1\ldots L \quad (2)$$
$$z_\ell = MLP(LN(z'_\ell)) + z'_\ell\ell = 1\ldots L \quad (3)$$
$$y = LN(z_L^0) \quad (4)$$

The layer normalization, called "LN", standardizes the training samples, to ensure the output is not affected by the number of features. The MSA, which means multihead self-attention, involved standard self-attention which is a common building block for neural architectures [25]. And **q**, **k**, and **v** are three different matrices.We calculate a weighted sum over all values **v** in the sequence for every single element in an input sequence $z \in \mathbb{R}^{N\times D}$. The attention weights A_{ij} are based on the pairwise similarity between two elements of the sequence and their respective query q^i and key k^j representations.

$$[q, k, v] = zU_{qkv}U_{qkv} \in \mathbb{R}^{D\times 3D_h} \quad (5)$$
$$A = soft\max(qk^T/\sqrt{D_h})A \in \mathbb{R}^{N\times N} \quad (6)$$
$$SA(z) = Av \quad (7)$$

The self-attention (SA), called "heads", will be operated **k** times in parallel. And their results will be concatenated and projected. To retain the calculation and number of parameters constant when k is changing, D_h is typically set to D/k.

$$MSA(z) = [SA_1(z); SA_2(z); \cdots; SA_k(z)]U_{msa}$$
$$U_{msa} \in \mathbb{R}^{k\cdot D_h\times D} \quad (8)$$

The MAE decoder has another series of Transformer blocks. And the input is the full set of tokens composed of encoded visible patches and mask tokens. See Figure 3. Each mask token is a shared, learned vector that indicates the presence of a missing patch to be predicted [28]. And all tokens will add positional embeddings in this full set. Moreover, mask tokens would have no information about their location in the image [29]. Figure 5 presents the detail of the Transformer encoder.

In summary, the whole process consists of three parts. And the pre-training task is the first step. The pre-training task's random masking of black patches (Accounting for 75% of the total) will be reconstructed by the MAE model, as seen in Figure 3. By completely reconstructing the two-dimensional matrix, the MAE model can learn the latent information there. This can be seen as getting to know one another by reading one other's postcards. This is the most vital part and the central idea of the MAE model. The next parts, training and forecasting, are thus in line with the traditional deep learning method. The pre-training system and the other (the training and prediction system) are two crucial subsystems that make up the entire model. Upon completion of the pre-training task, the model will activate a different mechanism during the formal training. Depending on whether it is a pre-training task or a formal training task, this switch can be manually operated. This is a point that may be confusing.

Because of this, the pre-training task with the masked mechanism is essential to comprehending the entire calculation process, and this article's application of it to aero-engine vibration is innovative.

V. CASE VALIDATION

In this section, we will briefly present the setting of some hyperparameters. And then the feasibility and applicability of forecasting aero-engine vibration signals will be demonstrated in terms of different aero-engine types and parameters, one by one. It should be noted that all models are fully pre-trained and trained in our experiments. And the model with

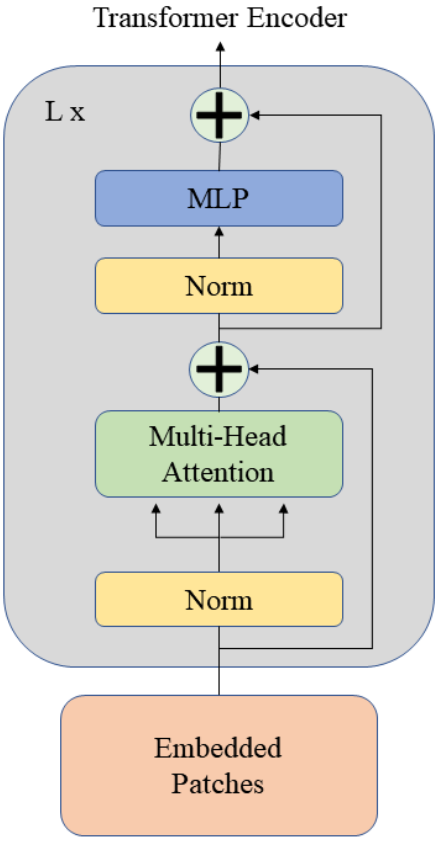

FIGURE 5. Transformer encoder.

TABLE 3. Parameters of cosine annealing lr.

Parameter	Meaning
η^i_{max}	Maximum learning rate
η^i_{min}	Minimum learning rate
T_{cur}	Current epoch
T_i	Number of periods

the smallest error of the test datasets in the training process will be selected for testing. Then, some offsets will be added to the test datasets and ten tests that are equal to the number of our prediction steps will be carried out, and the average of these results will be regarded as the final result. Therefore, the X-axis difference is caused by the order of test data in this paper. The purpose of our study is to forecast the future signals of vibration. As a result, we use mean square error (MSE) as the performance measure of our model.

$$\frac{1}{m}\sum_{i=1}^{m}(y_i - \hat{y_i})^2 \tag{9}$$

A. HYPERPARAMETERS SETTING

In this case study, we proposed a modified MAE model that could fit our aim properly. In this work, the depth of encoders are 12, and the decoder depth we used are 4.

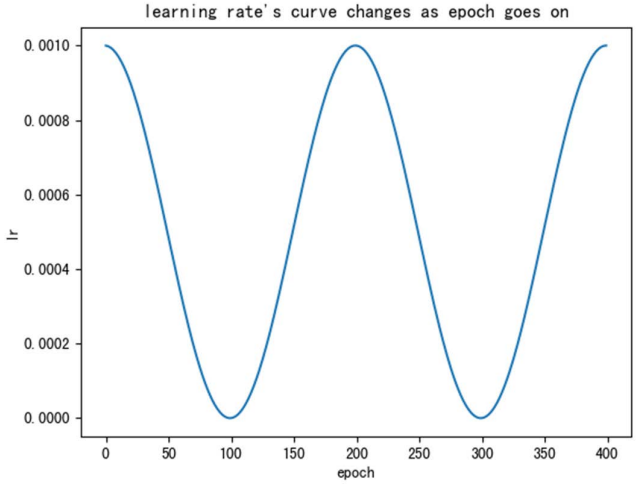

FIGURE 6. Cosine annealing LR.

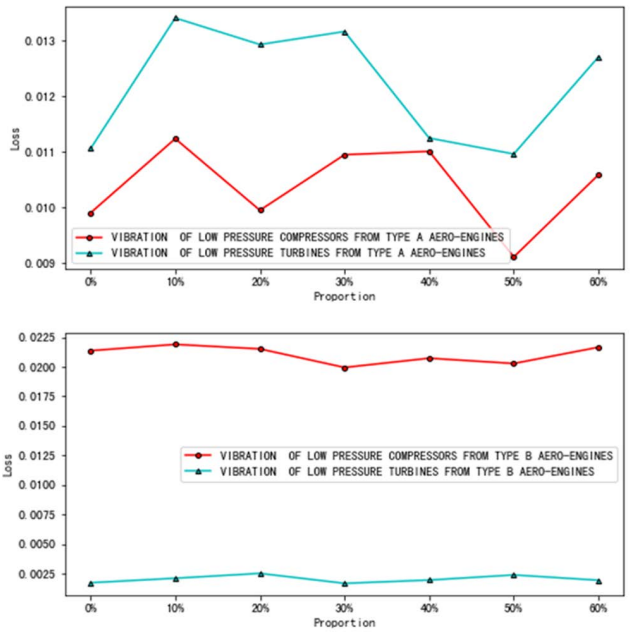

FIGURE 7. Comparison of pre-training tasks.

The embedding has dimensionality embed_dim = 512 and decoder_embed_dim = 256. Others are default. The original dimension of output is 1000, and we add two linear layers to the rear. This technique might make the model fit the vibration function better. The dimension of linear layers are (1000, 512) and (512, 10), because the expected steps are 10. We used the AdamW [31] optimizer with $\beta_1 = 0.9$, $\beta_2 = 0.95$ and weight_decay = 0.05 during pre-training. And we employ $\beta_1 = 0.9$, $\beta_2 = 0.999$ and weight_decay = 0.05 during downstream tasks. We varied the learning rate over the course of training, according to the formula [32]:

$$\eta_{lr} = \eta^i_{\min} + 0.5 \times (\eta^i_{\max} - \eta^i_{\min}) \times (1 + (\cos\frac{T_{cur}}{T_i}\pi)) \tag{10}$$

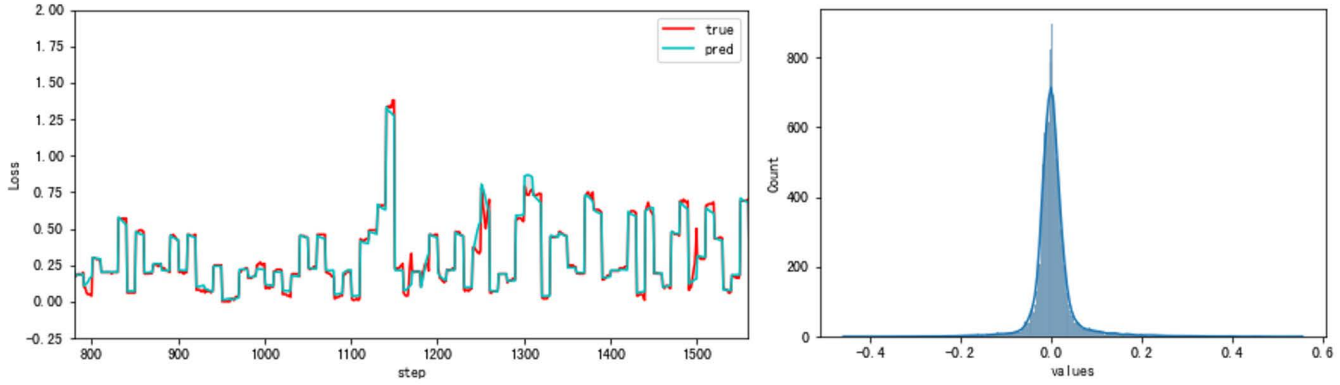

FIGURE 8. Results of SENet.

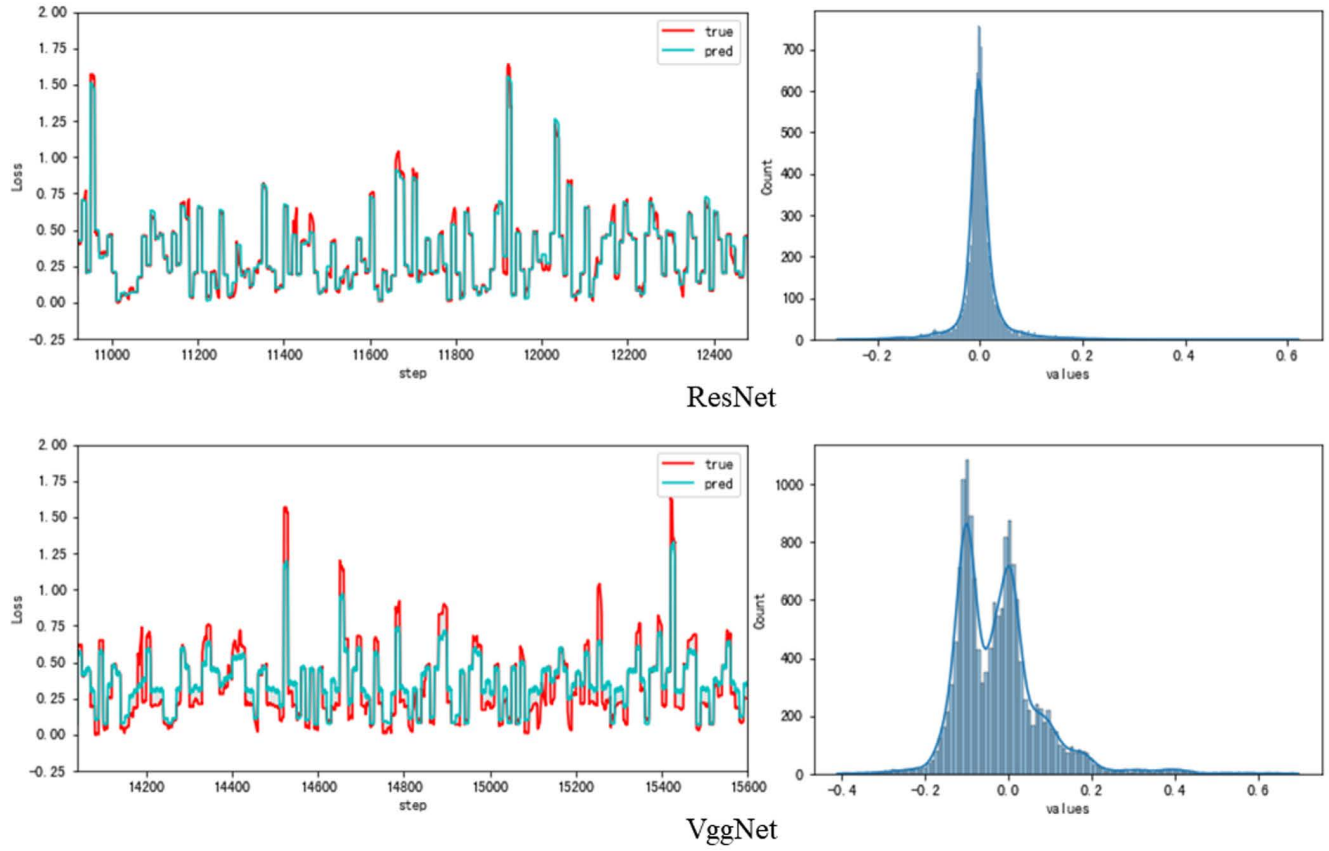

FIGURE 9. Results of ResNet and VggNet.

The strategy of learning can be defined as Cosine Annealing LR. Figure 6 shows the trend of this method and the table below illustrates the meaning of these parameters above.

Other hyperparameters, learning rate, epochs, and batch size, will be set as 0.0002, 400, 64 during pre-training and 0.0001, 200, 64 during fine-tuning.

Furthermore, in order to select the most appropriate proportion of pre-training data, comparisons are carried out as shown in Figure 7. As a result, 50% and 30% of the data will be chosen to pretrain the Type A and Type B aero-engine parameters, respectively.

B. VIBRATION SIGNALS OF LOW PRESSURE COMPRESSORS FROM TYPE A AERO-ENGINES

In this part, the vibration signal of low pressure compressors from Type A aero-engines is mainly used as our study object.

It should be noted that the unit of vibration level predicted in this paper is MILS.DA, so the numerical result forecasted in subsequent experiments is the square of this unit, while the Y-axis of the trend chart is this unit. And the gray area between different curves is the loss (the difference between the true and the forecasted). In addition to evaluating the MAE model, ResNet18 [33], VggNet18 [34] and

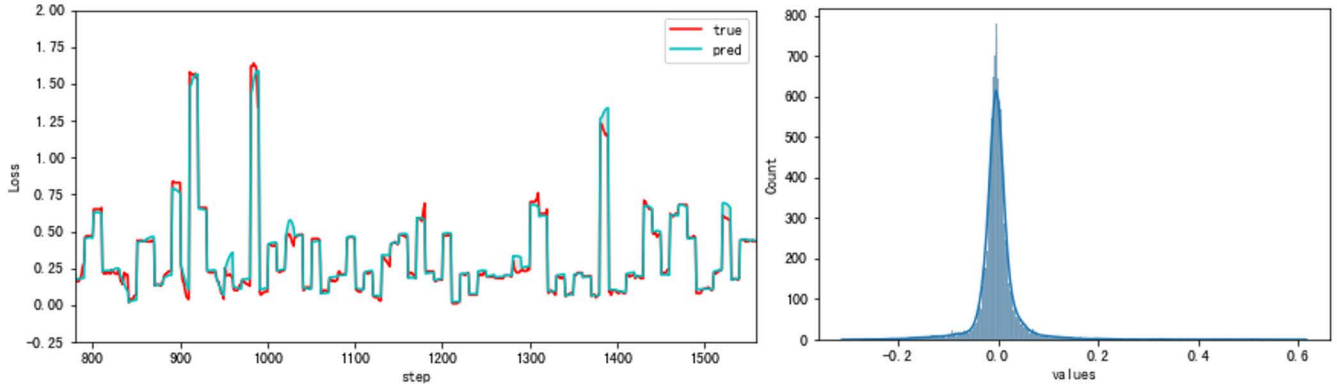

FIGURE 10. Results of ConvNeXt.

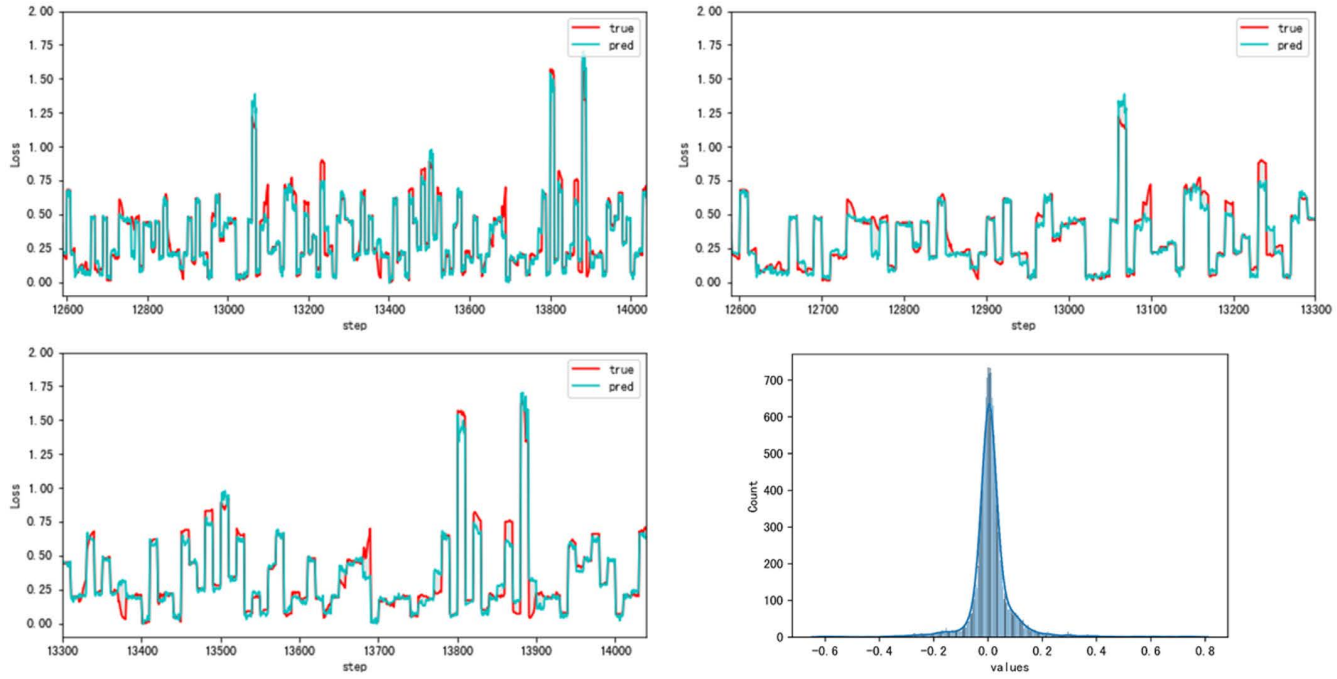

FIGURE 11. Results of the MAE model.

ConvNeXt18 [35] are also used to test the feasibility of prediction, as well as the results of errors are analyzed. It should be noted that the ConvNeXt model is the modernization of the ResNet model. A cutting-edge and potent algorithm is the ConvNeXt model, which is superior to Swin Transformer [36] and more advanced. Table 4 shows the results of these models. And Figures 8 to 11 present the details of the forecast. Meanwhile, Figure 12 shows the results without pretraining. It is not difficult to conclude from the below results that the ResNet model is the best and the VggNet model the worst. In addition, the result of the MAE model with pretraining is better than the one without pretraining. We believe that the MAE model used in this paper is a greatly complex model with a large scale of internal parameters, while the datasets used in our experiments are only a million scale.

TABLE 4. Comparison of different algorithms.

Model	Loss (MSE)
MAE	0.009116
MAE without pretraining	0.009908
SENet	0.002392
ResNet	0.002151
VggNet	0.011761
ConvNeXt	0.002481

Therefore, the MAE model could not obtain sufficient pretraining and training, which could lead to prediction results that are inferior to the light model (SENet18, ResNet18, and ConvNeXt18). Nevertheless, our experiments still proved the feasibility of forecasting aero-engine vibration signals. This

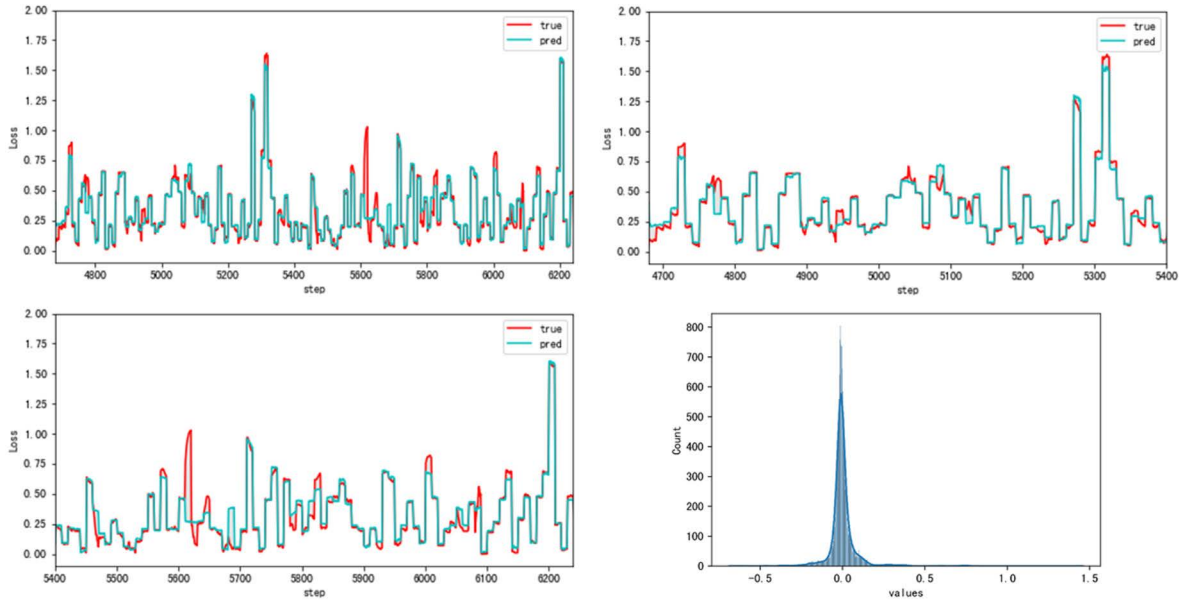

FIGURE 12. Results of the MAE model without pre-training.

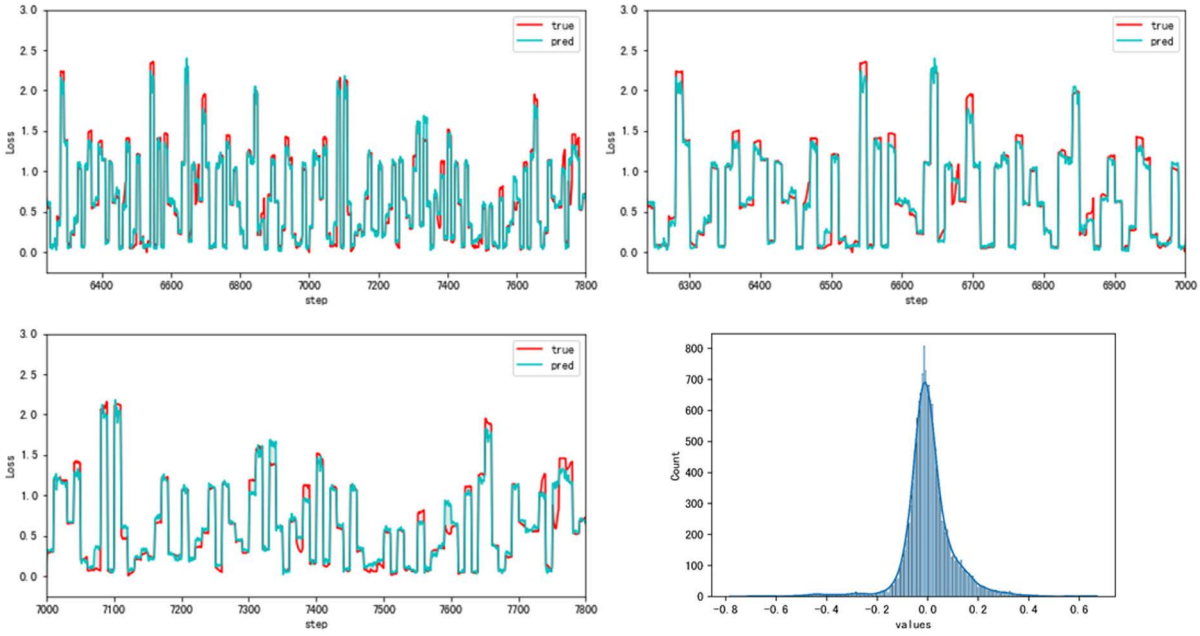

FIGURE 13. Forecast results of the vibration signal of low pressure turbines from Type A aero-engines.

is the most important goal we need to reach. In addition, it can be seen from Figure 11 and Figure 12 that the MAE model with pretraining could better track and forecast the conventional and instantaneous changes of vibration signals.

C. VIBRATION SIGANLS OF LOW PRESSURE TURBINES FROM TYPE A AERO-ENGINES AND VIBRATION LEVELS OF HIGH PRESSURE COMPRESSORS FROM TYPE B AERO-ENGINES

In this part, the vibration signal of low pressure turbines from Type A aero-engines and the vibration signal of high pressure compressors from Type B aero-engines are mainly used as our study object. This part, the applicability of forecasting aero-engines vibration will be verified. Figure 13 and Figure 14 present the results of prediction respectively. The experimental results show that not only the compressor and the turbine vibration signals can be predicted but also the vibration signals from various types of aero-engines. And the results of Figure 13 perform better than Figure 14. In combination with the result of Part D, we believe that the parameters used to forecast the vibration signal of Type A aero-engines are sufficient, hence the MAE model could fully learn the

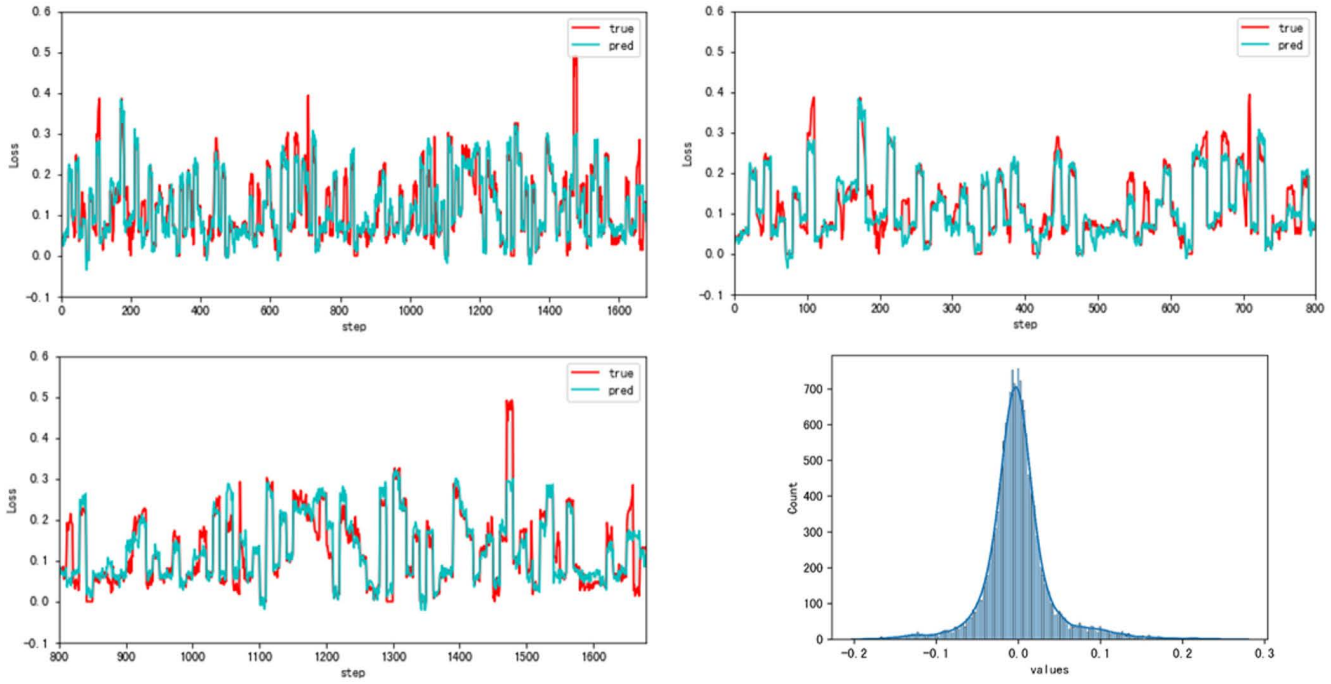

FIGURE 14. Forecast results of the vibration signal of high pressure compressors from Type B aero-engines.

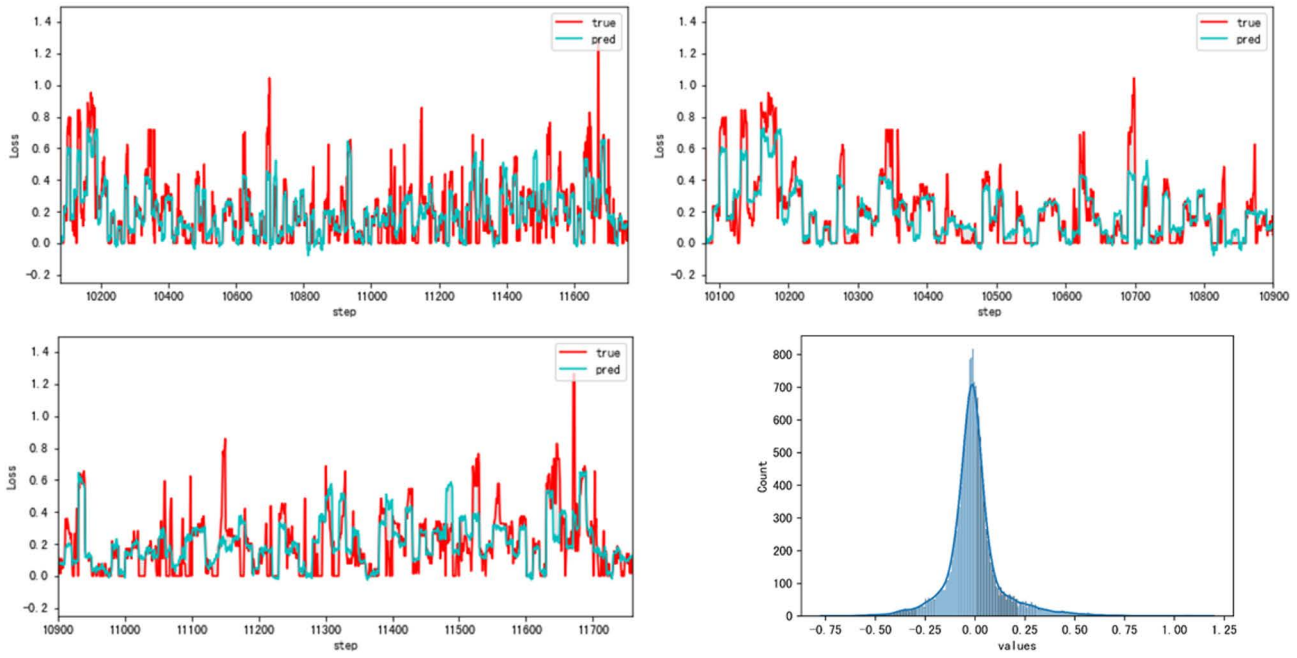

FIGURE 15. Forecast results of the vibration signal of low pressure compressors from Type B aero-engines.

time sequence relation between various parameters and the characteristics of vibration changes, hence it could output better prediction results from Type A aero-engines. But from experiments with the Type B aero-engines, it can be seen that the required training conditions are not particularly adequate. Therefore, some vital vibration features could not be learned by the MAE model, resulting in relatively poor forecast outputs.

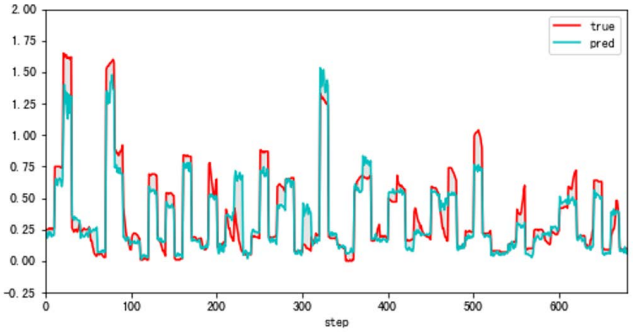

FIGURE 16. The transition state (the low pressure compressor, Type A).

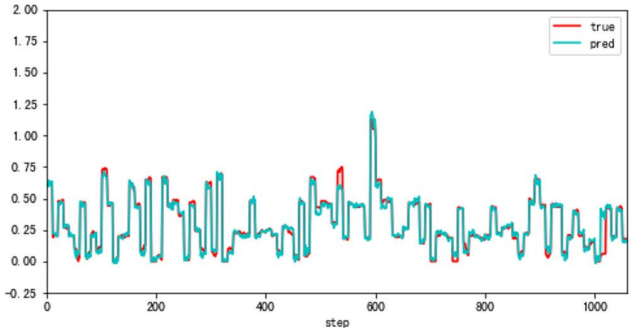

FIGURE 17. The steady state (the low pressure compressor, Type A).

D. VIBRATION SIGNALS OF LOW PRESSURE COMPRESSORS FROM TYPE B AERO-ENGINES

In this part, the vibration signal of low pressure compressors from Type B aero-engines is mainly used as our study object. Contrary to the previous prediction with high accuracy, the vibration trend forecast in this part is only acceptable. Figure 15 shows the results. It is clear from Figure 15 that the MAE model could only forecast the overall vibration tendency, but it cannot track and predict the correct value that should be forecasted in the face of great fluctuations and sudden changes. As a result, this level of forecast accuracy could not be accepted in real industrial practices. The reason why the results are not relatively acceptable in this vibration predictive experiment could be that the strongly vibration-related features are not sufficient to forecast this vibration signal. Therefore, it is unavoidable that the prediction will contain relatively large errors under such inadequate conditions. This is the same as Part C. Despite the fact that choosing parameters is not the main emphasis of this essay, it makes an effort to be thorough and choose as many pertinent parameters as it can. As a result, there might be additional factors, such mechanical ones, that cause rather substantial prediction errors. This research does not attempt to go into great detail on this, though, as it deviates from the main goal of the paper, which is to explore the viability and applicability of forecasting the aero-engine vibration. As a result, we intend to start a new topic in the relevant study that follows to concentrate on the factors that influence the forecast accuracy.

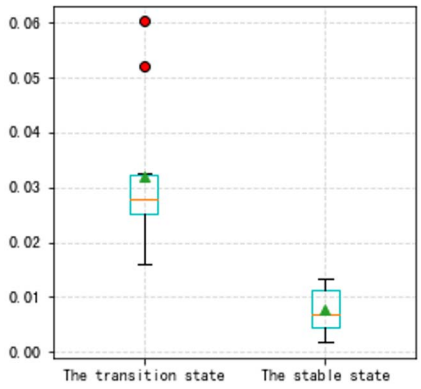

FIGURE 18. The box plot of the two states (the low pressure compressor, Type A).

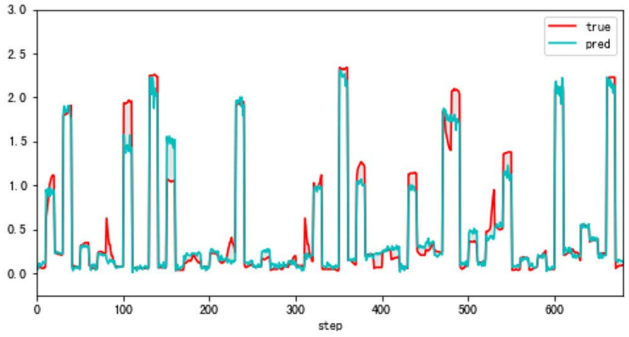

FIGURE 19. The transition state (the low pressure turbine, Type A).

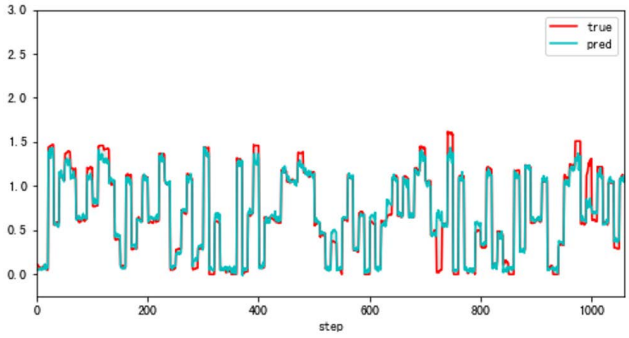

FIGURE 20. The steady state (the low pressure turbine, Type A).

E. AERO-ENGINE STATES ANALYSIS

In this Part, to make our thoughts more reasonable and convincing, two groups of state experiments on the Type A aero-engine's low pressure compressors and low pressure turbines are carried out in this part. As mentioned above, we have performed pertinent experimental verification for the aero-engine types here. The datasets we used in this part are test datasets that have been divided into transition state and steady state portions. It should be noted that when an airplane is in flight, the aero-engine is in its steady condition for a longer period of time than it is in its transitional state. Therefore, steady state datasets are bigger than transition

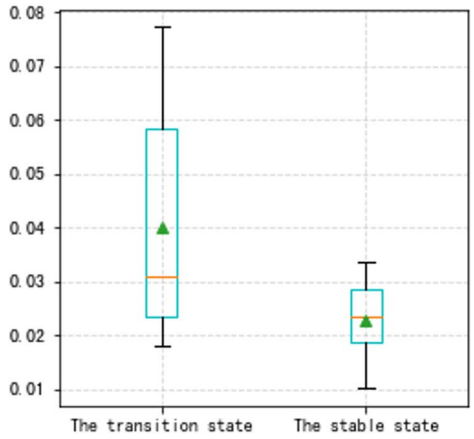

FIGURE 21. The box plot of the two states (the low turbine compressor, Type A).

state datasets. As can be shown that regardless of whether the compressor or the turbine is forecast, the transition state prediction error is higher than the steady state forecasted error. But the cost of forecasting the transition state of the aero-engine vibration is still acceptable. And the MAE model can track its changes in time.

From Figure 19 to Figure 21, figures present forecasted results for the Type A aero-engine's low pressure turbines. And results are similar to the low pressure compressor. The model can give relatively accurate forecasted outcomes as well. This leads to an extremely crucial conclusion that even in the most complicated state, the transition state, the future trend of the system and the quick shift in the degree may both be reliably and accurately forecasted. In addition, it is reasonable to believe that through our strategy of feeding the MAE model with random extracting datasets, the MAE model itself has learned the important features of distinguishing the transition state and steady state according to the input data. When the identification job is done, an accurate forecast value can be output.

VI. CONCLUSION

Aiming at the feasibility of forecasting aero-engine vibration level, this paper uses an advanced and powerful deep learning algorithm in other domains to forecast the aero-engine vibration, which means the changes in aero-engine vibration have been forecasted based on the actual flight datasets gathered by aircraft data acquisition systems. It is an innovative application that the MAE model is used in the area of time series prediction. And the forecast of the aero-engine vibration is also a leading leap in the domain of aero-engine vibration research. The experiments of aero-engine vibration prediction have been tested by substantial and sufficient experiments based on real flight datasets. Therefore, the validity of this paper's results can be guaranteed. More importantly, in order to make our results more convincing and reliable, experiments on different types of aero-engines and different aero-engine states have been carried out, which is very rare in previous aero-engine vibration research. Therefore, the applicability is assured either.

The study has shown that ① forecasting the vibration signal of aero-engines is feasible to some extent. Compared with the previous research on fault diagnosis and prognosis, the MAE model could forecast future vibration changes and might track the sudden change and fluctuations of vibration signals. Meanwhile, the latent interaction of parameters can be learned deeply in the process of the pre-training task. Because the established pattern is a normal operating pattern when engine vibration is irregular, we can compare the forecasted value against the actual value to provide early warning, which could contribute to flight safety. ② The applicability of the forecast is also verified above. It is possible to forecast not only the future trend of the various vibration signals but also the vibration signal of different types of aero-engines. Even the vibration signals of various aero-engine systems could be forecasted. This achievement is of great importance for the understanding and the design of the aero-engine and other vibration systems in other domains. ③ In addition, whether the model can identify different aero-engine running states and make accurate predictions are also verified in this article. Therefore, there are enough reasons to believe that a sufficiently complex algorithm model can learn different states' features at the same time when the amount of data is ample. ④ By studying multi-parameter fusion, it is known that the complexity of the vibration system in the aero-engine. Therefore, this result could also be used to check which parameters can affect the running of the aero-engine vibration system. Meanwhile, this result shows that the influence of multiple parameters should be considered as much as possible when studying complex vibration systems in aero-engines. In the past, most research has focused on a single vibration parameter, simplifying the vibration system of the engine. However, vibration is affected by many factors.

It should be emphasized that the model will take into account both the trend of other parameters and the future tendency of the vibration signals when making predictions. As a result, the model may become inert and fail to take the trend in parameter development into account. Additionally, the forecast's capacity will be diminished when significant variations and actual changes occur. Especially if the aero-engine status changes while it is really running. As a result, this will be the subsequent stage in the forecasting process where future information from other parameters is taken into account. The choice of parameters may possibly be a significant concern in the future.

ACKNOWLEDGMENT

(Cunjiang Xia and Yuyou Zhan contributed equally to this work.)

REFERENCES

[1] Y. Shi, J. Zhao, and Y. Liu, "Switching control for aero-engines based on switched equilibrium manifold expansion model," *IEEE Trans. Ind. Electron.*, vol. 64, no. 4, pp. 3156–3165, Apr. 2017.

[2] C. Sun, Z. He, H. Cao, Z. Zhang, X. Chen, and M. J. Zuo, "A non-probabilistic metric derived from condition information for operational reliability assessment of aero-engines," *IEEE Trans. Rel.*, vol. 64, no. 1, pp. 167–181, Mar. 2014.
[3] Civil Aviation Resources Website. (Sep. 8, 2018). *Statistics Report on China Civil Aviation Safety Information From January to June*. [Online]. Available: http://news.carnoc.com/list/461/461183.html
[4] H. Wang, "A survey of maintenance policies of deteriorating systems," *Eur. J. Oper. Res.*, vol. 139, no. 3, pp. 469–489, Jun. 2002.
[5] D. I. Cho and M. Parlar, "A survey of maintenance models for multi-unit systems," *Eur. J. Oper. Res.*, vol. 51, no. 1, pp. 1–23, Mar. 1991.
[6] J. Lee and H. Wang, "New technologies for maintenance," in *Complex System Maintenance Handbook*. London, U.K.: Springer, 2008, pp. 49–78.
[7] M. Xiong, H. Wang, Q. Fu, and Y. Xu, "Digital twin–driven aero-engine intelligent predictive maintenance," *Int. J. Adv. Manuf. Technol.*, vol. 114, nos. 11–12, pp. 3751–3761, Jun. 2021.
[8] R. Wang, M. Liu, and Y. Ma, "Fault estimation for aero-engine LPV systems based on LFT," *Asian J. Control*, vol. 23, no. 1, pp. 351–361, Jan. 2021.
[9] X. Xie, "Research on performance assessment and degradation prediction of aeroengine," Ph.D. dissertation, Harbin Inst. Technol., Harbin, China, 2016.
[10] H. Zhang, X. Chen, X. Zhang, B. Ye, and X. Wang, "Aero-engine bearing fault detection: A clustering low-rank approach," *Mech. Syst. Signal Process.*, vol. 138, Apr. 2020, Art. no. 106529.
[11] Z. He, H. Shao, Z. Ding, H. Jiang, and J. Cheng, "Modified deep autoencoder driven by multisource parameters for fault transfer prognosis of aeroengine," *IEEE Trans. Ind. Electron.*, vol. 69, no. 1, pp. 845–855, Jan. 2022.
[12] T. Lin, G. Chen, W. Ouyang, Q. Zhang, H. Wang, and L. Chen, "Hyperspherical distance discrimination: A novel data description method for aero-engine rolling bearing fault detection," *Mech. Syst. Signal Process.*, vol. 109, pp. 330–351, Sep. 2018.
[13] Y. Lei, J. Feng, K. Detong, L. Jing, and X. Saibo, "Opportunities and challenges of mechanical intelligent fault diagnosis under big data," *J. Mech. Eng.*, vol. 54, no. 5, pp. 94–104, 2018.
[14] T. Kohonen, "An introduction to neural computing," *Neural Netw.*, vol. 1, no. 1, pp. 3–16, 1988.
[15] K. Greff, R. K. Srivastava, J. Koutnìk, B. R. Steunebrink, and J. Schmidhuber, "LSTM: A search space Odyssey," *IEEE Trans. Neural Netw. Learn. Syst.*, vol. 28, no. 10, pp. 2222–2232, Oct. 2017.
[16] S. Albawi, T. A. Mohammed, and S. Al-Zawi, "Understanding of a convolutional neural network," in *Proc. Int. Conf. Eng. Technol. (ICET)*, Aug. 2017, pp. 1–6.
[17] D. Yongfeng, Y. Sun, L. Gao, P. Han, and H. Ji, "Fault diagnosis method based on improved one-dimensional convolution and bidirectional long short-term memory neural network," *J. Comput. Appl.*, vol. 42, no. 4, p. 1207, 2021.
[18] H. Shao, H. Jiang, X. Li, and T. Liang, "Rolling bearing fault detection using continuous deep belief network with locally linear embedding," *Comput. Ind.*, vol. 96, pp. 27–39, Apr. 2018.
[19] X. Li, W. Zhang, and Q. Ding, "Cross-domain fault diagnosis of rolling element bearings using deep generative neural networks," *IEEE Trans. Ind. Electron.*, vol. 66, no. 7, pp. 5525–5534, Jul. 2019.
[20] J. Xu and L. Xu, "Health management based on fusion prognostics for avionics systems," *J. Syst. Eng. Electron.*, vol. 22, no. 3, pp. 428–436, Jun. 2011.
[21] CFMI Customer Training Center, *Training Manual CFM56-7B engine systems*, CFMI, Cincinnati, OH, USA, 2012.
[22] CFM Company, *CFM56-7B Advanced Engine System*, GE Customer training center, Cincinnati, OH, USA, 2016, pp. 99–130.
[23] N. A. Jalil, H. J. Hwang, and N. M. Dawi, "Machines learning trends, perspectives and prospects in education sector," in *Proc. 3rd Int. Conf. Educ. Multimedia Technol. (ICEMT)*, 2019, pp. 201–205.
[24] T. Mitchell, *Key Ideas in Machine Learning*. Pittsburgh, PA, USA: Carnegie Mellon Univ., 2017.
[25] A. Vaswani, N. Shazeer, N. Parmar, J. Uszkoreit, L. Jones, A. N. Gomez, Ł. Kaiser, and I. Polosukhin, "Attention is all you need," in *Proc. Adv. Neural Inf. Process. Syst.*, vol. 30, 2017, pp. 1–11.
[26] A. Radford et al. (Jun. 11, 2018). *Improving Language Understanding With Unsupervised Learning*. [Online]. Available: https://openai.com/blog/language-unsupervised/
[27] J. Howard and S. Ruder, "Universal language model fine-tuning for text classification," 2018, *arXiv:1801.06146*.
[28] J. Devlin, M.-W. Chang, K. Lee, and K. Toutanova, "BERT: Pre-training of deep bidirectional transformers for language understanding," 2018, *arXiv:1810.04805*.
[29] K. He, X. Chen, S. Xie, Y. Li, P. Dollár, and R. Girshick, "Masked autoencoders are scalable vision learners," 2021, *arXiv:2111.06377*.
[30] A. Dosovitskiy, L. Beyer, A. Kolesnikov, D. Weissenborn, X. Zhai, T. Unterthiner, M. Dehghani, M. Minderer, G. Heigold, S. Gelly, J. Uszkoreit, and N. Houlsby, "An image is worth 16×16 words: Transformers for image recognition at scale," 2020, *arXiv:2010.11929*.
[31] I. Loshchilov and F. Hutter, "Decoupled weight decay regularization," 2017, *arXiv:1711.05101*.
[32] A. Hundt, V. Jain, and G. D. Hager, "SharpDARTS: Faster and more accurate differentiable architecture search," 2019, *arXiv:1903.09900*.
[33] K. He, X. Zhang, S. Ren, and J. Sun, "Deep residual learning for image recognition," in *Proc. IEEE Conf. Comput. Vis. Pattern Recognit. (CVPR)*, Jun. 2016, pp. 770–778.
[34] K. Simonyan and A. Zisserman, "Very deep convolutional networks for large-scale image recognition," 2014, *arXiv:1409.1556*.
[35] Z. Liu, H. Mao, C.-Y. Wu, C. Feichtenhofer, T. Darrell, and S. Xie, "A ConvNet for the 2020s," in *Proc. IEEE/CVF Conf. Comput. Vis. Pattern Recognit. (CVPR)*, Jun. 2022, pp. 11976–11986.
[36] Z. Liu, Y. Lin, Y. Cao, H. Hu, Y. Wei, Z. Zhang, S. Lin, and B. Guo, "swin Transformer: Hierarchical vision transformer using shifted Windows," in *Proc. IEEE/CVF Int. Conf. Comput. Vis. (ICCV)*, Oct. 2021, pp. 10012–10022.

CUNJIANG XIA received the M.E. degree in aeronautical engineering from Northwestern Polytechnical University, Shan'xi, China, in 2005. He is currently a Full Professor with the Civil Aviation Flight University of China, China. He work for IEEE committees and publications. His main research interests include the technology of aeroengine control and maintenance.

YUYOU ZHAN is currently pursuing the M.E. degree in aeronautical and astronautical science and technology with the College of Aeronautical Engineering, Civil Aviation Flight University of China, Si'chuan, China. His research interests include aeroengine fault analysis, artificial intelligence, and data mining.

YAN TAN received the master's degree in aviation engineering from Northwestern Polytechnical University, Xi'an, China, in 2005. She is currently a Full Professor with the Aero Engine Maintenance Training Center, Civil Aviation Flight University of China. Her main research interests include fault diagnosis and health management, big data analysis, and maintenance support of aeroengine.

WENQING WU is currently pursuing the B.E. degree in aircraft manufactureing engineering with the College of Aeronautical Engineering, Civil Aviation Flight University of China, Si'chuan, China. Her research interests include aircraft fault diagnosis, artificial intelligence, and data mining.